arXiv:cond-mat/0601575v1 [cond-mat.str-el] 25 Jan 2006

Infrared observation of the Hund's mechanism in an electron-doped manganite

A. Nucara[1], P. Calvani[1], F. Crispoldi[1], D. Sali[1], S. Lupi[1], C. Martin[2], and A. Maignan[2]
[1] *"Coherentia"-INFM and Dipartimento di Fisica,*
Università di Roma "La Sapienza", Piazzale A. Moro 2, I-00185 Roma, Italy and
[2] *Laboratoire CRISMAT-UMR 6508 ENSICAEN, 6, Bd. Maréchal Juin, 14050 Caen, France*

(Dated: February 6, 2008)

In the mid-infrared absorption of $Sr_{1-x}Ce_xMnO_3$ at low electron doping ($x = 0.05$), a band at 0.3 eV is fully replaced by another one at 0.9 eV as the system becomes antiferromagnetic (AF) of type G. A weaker effect occurs at $x = 0.10$ for an AF phase of type C. One thus directly measures the electron hopping energies for spin parallel and anti-parallel to that of the host ion. The Hund's, crystal-field, and Jahn-Teller splittings for the Mn^{3+} ions in a Mn^{4+} matrix, can also be derived.

PACS numbers: 75.50.Cc, 78.20.Ls, 78.30.-j

I. INTRODUCTION

The close interplay between charge dynamics and magnetism is the basic feature of the manganites $A_{1-x}B_xMnO_3$ (A = La,Nd and B = Sr,Ca). Generally speaking, these perovskites show poor conductivity in the paramagnetic (PM) phase at high T, metallic conduction in the ferromagnetic (FM) phase, charge localization and (often) ordering in the antiferromagnetic (AF) phase at low T. The metallic FM phase is explained by the double-exchange mechanism [1, 2], with corrections [3] for the Jahn-Teller distortion that the oxygen octahedra around the Mn^{4+} ions experience as they receive an additional electron. The polaronic nature of the carriers is confirmed by the observation of characteristic bands in the mid-infrared [4, 5, 6, 7] which depend both on doping and temperature.

The insulating character of the AF phases is basically explained by the Hund's mechanism. Each Mn^{4+} ion has three electrons t_{2g}, and spin $S = 3/2$. An Mn^{3+} ion at site i has an additional electron e_g with spin $s = 1/2$ and Hund's energy $-J_H\vec{s}\cdot\vec{S}_i = -(1/2)J_HS$. Let $\vec{S}_i$ be up and the system slightly electron-doped, so that the 6 nearest neighbors at sites j are all Mn^{4+} with $S_j = S$. In the high-temperature PM phase the $\vec{S}_j$ are randomly oriented. One at least will be up, and will allow for a $i - j$ hopping with no change in the Hund's energy (Fig. 1-a). As the j site is initially undistorted, the electron will then pay an energy

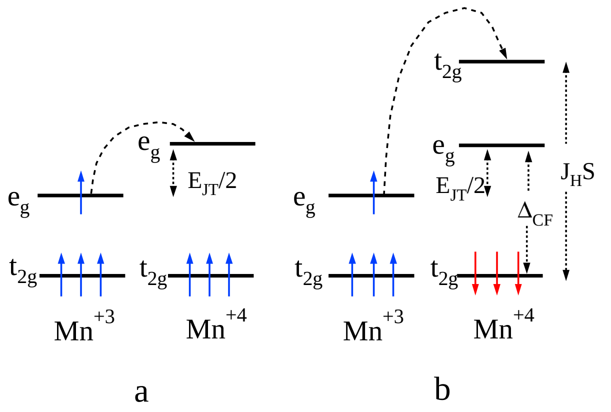

FIG. 1: (Color online) Energy diagram describing the hopping of an electron with spin parallel (a) or antiparallel (b) to that of the Mn^{4+} ion.

$$E_{\uparrow\uparrow} = E_{JT}/2\,, \tag{1}$$

where E_{JT} is the $e_g - e_g$ Jahn-Teller splitting. Its value may include corrections for the "breathing" distortion of the oxygen octahedra around Mn^{4+} [8, 9], or for the binding energy of a magnetic polaron which forms around the hopping electron [10].

In an AF phase of type G all the $\vec{S}_j$ are antiparallel to $\vec{s}$. If the system enters such phase below the Néel temperature T_N, the Hund's final energy becomes $+(1/2)J_HS$ and the hopping electron will pay an extra-energy J_HS. According to calculations for $CaMnO_3$, based on the Local Density Approximation[11], the lowest antiparallel state is t_{2g}. In this case the energy diagram is that of Fig. 1-b and

$$E_{\uparrow\downarrow} = E_{JT}/2 + J_HS - \Delta_{CF}\,. \tag{2}$$

Here J_HS is the Hund's splitting between two t_{2g} states with antiparallel spin and Δ_{CF} is the t_{2g} - e_g crystal-field splitting at j. If instead the lowest Mn^{4+} state with antiparallel spin were e_g, the hopping energy would simply be $E_{\uparrow\downarrow} = E_{JT}/2 + J_HS$.

As $E_{\uparrow\downarrow}$ is much larger than the thermal energy available below T_N, the e_g electron will remain localized at i. In an AF phase of type C on the other hand, both $\vec{S}_j$ above and below $\vec{S}_i$ are up while the four in-plane ones are down [12]. The electron will pay just $E_{\uparrow\uparrow}$ to move along the c axis, a much higher $E_{\uparrow\downarrow}$ to move in the plane. Nevertheless, it has been shown that an AF phase of type C does not provides a one-dimensional metal in manganites, due to correlation effects [13]. The opposite situation is encountered in an AF phase of type A, where the out-of-plane spins are parallel to S_i and the in-plane ones are antiparallel. The FM planes of the A phases, in manganites are close to a metallic planar instability[12].

According to the band calculations of Ref. 11, in the all-Mn^{4+} system CaMnO$_3$ J_HS varies between 1.7 and 2.8 eV throughout the Brillouin zone. Up to now, experimental evaluations of J_HS in the FM or PM phases of hole-doped manganites were extracted from bands in the visible or UV range and vary from 0.9 through 3.4 eV [7, 14, 15]. In the orbital-ordered, AF phase of the all-Mn^{3+} system LaMnO$_3$, $(1/5)J_HS$ is reported to be 0.5 eV [16].

Here we report a direct determination of $E_{\uparrow\uparrow}$ and $E_{\uparrow\downarrow}$ based on the abrupt transition, at T_N, from a regime of spin-parallel hopping to one of anti-parallel hopping. We show that, in a manganite at low electron dilution, this induces a spectacular effect in its mid-infrared absorption. This effect allows one to determine, with unprecedented precision, most of the energies involved in the above Equations. The experiment is performed on Sr$_{1-x}$Ce$_x$MnO$_3$ (SCMO), where Ce is in the +3 state [17] and provides the electrons, because: i) unlike the La-based manganites [18], it exhibits a good chemical stability at low doping; ii) it exhibits different AF phases and Néel temperatures for different x, and this will provide a good check of the results.

II. EXPERIMENT

Two polycrystalline, SCMO pellets have been studied here, having $x = 0.05$ and $x = 0.10$. For $x = 0.05$, room-temperature x-ray diffraction data are well fitted by the cubic Pm3m space group with lattice constant a = 0.38107 nm. For $x = 0.10$ the structure is tetragonal (I4/mcm) with $a = b = 0.53637$ nm and $c = 0.77481$ nm. Neither sample exhibits any trace of spurious hexagonal phases and only a small volume fraction (4 %) of the x = 0.10 sample is cubic, from pure SrMnO$_3$. This will not affect the optical measurements presented here, which will be focused on electronic transitions from e_g states, not occupied at the $x = 0$ composition.

The magnetic susceptibility $\chi(T)$ is shown for both samples in Fig. 2. Sharp maxima are found at T_{max} = 225 K and 325 K for $x = 0.05$ and 0.10, respectively. The peak at 325 K is reported to be observed also in Ref. 19 for the same x value, even if data are not shown. A shoulder appears in both samples at $T_{sh} < T_{max}$. Neutron scattering data show that the AF order is fully established below T_{sh}, which therefore is the effective Néel temperature [17]. In our samples, T_N is then 205 K for $x = 0.05$, 295 K for $x = 0.10$. The AF phase is of type G [20] at $x = 0.05$ (as at $x = 0$), of type C [21] at x = 0.10. This behavior is fully consistent with the general properties of manganites at high divalent dopant concentration (see, *e. g.*, Fig. 1 of Ref. 22). Between T_{max} and T_N there should be a mixed AF-FM phase, as found in Ca$_{0.82}$Bi$_{0.18}$MnO$_3$ in correspondence of a behavior for the magnetic susceptibility [23] quite similar to that of Fig. 2.

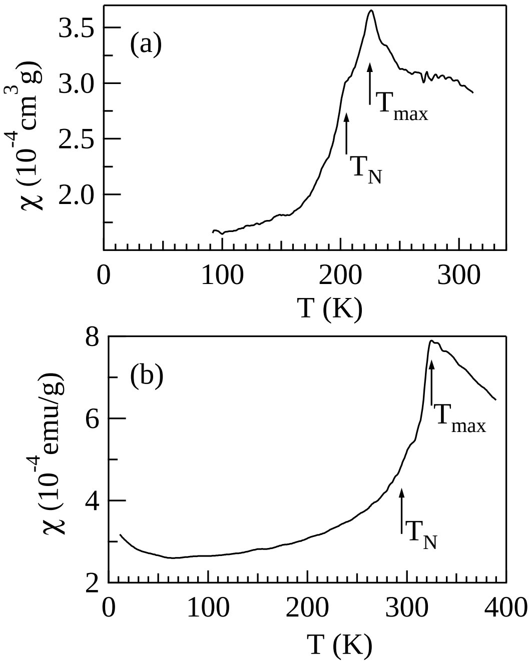

FIG. 2: Magnetic susceptibility vs. T of Sr$_{0.95}$Ce$_{0.05}$MnO$_3$ (a) and of Sr$_{0.90}$Ce$_{0.10}$MnO$_3$ (b). Neutron scattering data (see text) show that the sample in a) enters an AF phase of type G below $T_N \simeq 205$ K, the one in b) an AF phase of type C below $T_N \simeq 295$ K.

We have measured, for both $x = 0.05$ and 0.10, the reflectivity $R(\omega)$ of polycrystalline pellets of Sr$_{1-x}$Ce$_x$MnO$_3$, prepared and controlled as described in Ref. 17. $R(\omega)$ was measured at nearly normal incidence (8^0) on an accurately polished surface. The absence of "ghost" peaks in $R(\omega)$ around 0.1 eV, as those reported for certain single crystals after polishing [24], excludes appreciable surface damage to our polycrystalline pellets, where the radiation penetrates deeply due to their poor optical conductivity ($\approx 10^2$ Ω^{-1} cm^{-1} at all frequencies and temperatures, see below). In order to minimize errors due to residual irregularities of the surface, the reference was obtained by evaporating a metal film onto the sample (gold for $\omega < 14000$ cm^{-1}, silver between 14000 cm^{-1} and 20000 cm^{-1}). The results were then corrected for their real reflectivity. Data were collected by a rapid-scanning interferometer between 30 and 20000 cm^{-1} and by thermoregulating the samples within ± 2 K between 380 and 15 K. From 20000 to 40000 cm^{-1}, $R(\omega)$ was measured at room temperature with respect to a silver mirror by using a monochromator coupled to a charge-coupled device. The polycrystalline nature of the material may be source of errors, especially in the far infrared, if the transport properties are strongly anisotropic [25]. However, in the present case, the in-plane Mn-O(2) bond length differs from the orthogonal Mn-O(1) one by

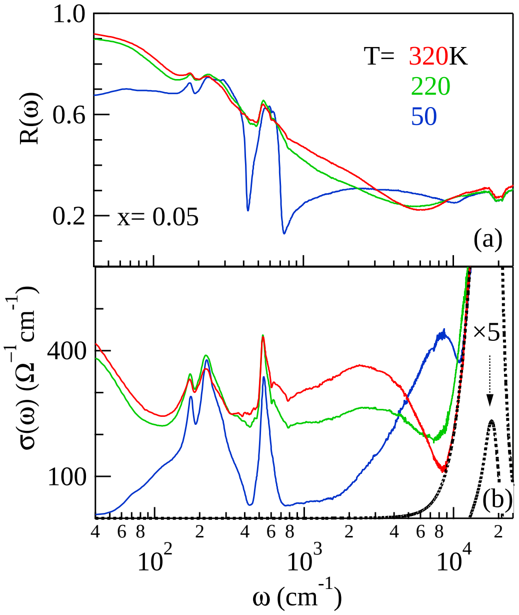

FIG. 3: (Color online) Reflectivity (a) and optical conductivity (b) of $Sr_{0.95}Ce_{0.05}MnO_3$.

less than 1.5 % [17]. Moreover, anisotropies in $\sigma(\omega)$, as those reported for SCMO in Ref. 22 above $x = 0.30$, are rigorously excluded for our sample with $x = 0.05$, where also the *AF* phase is isotropic (*G*). As the same bands are observed at $x = 0.10$, one can conclude that the latter spectra are also fully reliable.

III. RESULTS AND DISCUSSION

Both the reflectivity $R(\omega)$ and the resulting optical conductivity $\sigma(\omega)$ are shown in Fig. 3 for the 0.05 sample. Three main phonon lines, as predicted for the Pm3m structure of these perovskites [17], are observed at low ω. They are partially shielded at high T by a weak Drude contribution accounting for the poor dc conductivity of the PM phase. On the opposite side, the strong band at 18000 cm^{-1} is due to O-Mn charge transfer [26].

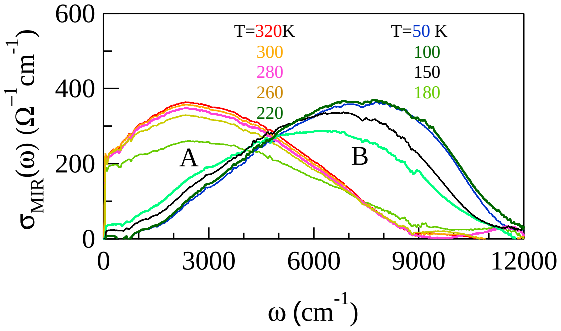

FIG. 4: (Color online) The optical conductivity of $Sr_{0.95}Ce_{0.05}MnO_3$ is subtracted of the contributions in the far infrared (Drude, phonon) and in the visible range, and reported at all temperatures. Below $T_N = 205$ K the *A* band at 0.3 eV is fully replaced by the *B* band at 0.9 eV.

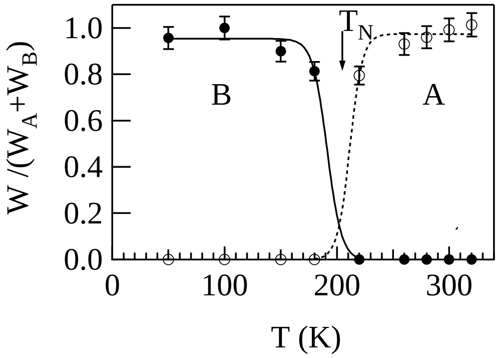

FIG. 5: Relative spectral weight vs. T, in $Sr_{0.95}Ce_{0.05}MnO_3$, of the *A* (circles) and *B* band (dots) of Fig. 4. The lines are guides to the eye and the arrow indicates the Néel temperature extracted from Fig. 2.

The usual sum rule on $\sigma(\omega)$ is fulfilled, provided that it is integrated up to 15000 cm^{-1}. However, in the mid-infrared range a broad band dramatically shifts towards higher energies when cooling the sample. In order to better study this effect, the imaginary part of the dielectric function $\epsilon_2(\omega) = (4\pi/\omega)\sigma(\omega)$ was fitted to a Drude-Lorentz model as in Ref. 4. Then, both the far-infrared contributions from phonons and Drude, and the tail of the strong band at high energy in Fig. 3 -b, were subtracted. In the resulting mid-infrared conductivity, reported in Fig. 4, $Sr_{0.95}Ce_{0.05}MnO_3$ shows in the PM phase a single band *A* peaked at 2500 cm^{-1}, or about 0.3 eV. At 220 K, as T_N is approached by cooling the sample, the peak energy does not change but its intensity decreases rapidly until, at 180 K, the *A* band is fully replaced by a *B* band peaked at $\sim$ 7500 cm^{-1}, or approximately 0.9 eV. The spectral weights W_A and W_B, obtained by integrating the $\sigma(\omega)$ of the corresponding bands, are plotted vs. temperature in Fig. 5. Therein, one can appreciate the on-off transfer of spectral weight from *A* to *B*, and check that it is triggered by the PM-AF transition at T_N.

Basing on the scenario described above, one can reasonably associate the *A* band of the PM phase with intersite transitions with $\vec{S}_i$ and $\vec{S}_j$ parallel. $E_{\uparrow\uparrow}$ in Eq. 1 is therefore 0.3 eV. The *B* band observed below T_N is instead due to the same transitions with $\vec{S}_i$ and $\vec{S}_j$ antiparallel, so that $E_{\uparrow\downarrow}$ in Eq. 2 is 0.9 eV. The fact that antiparallel hopping is not observed at all in the PM phase implies that therein the e_g electron tends to align the core spins of the neighboring Mn^{4+} ions, forming magnetic polarons. This is indeed predicted to occur [10] in the electron-doping region of $La_{1-x}Ca_xMnO_3$ with $x \lesssim 1$, which corresponds to the present case. Their

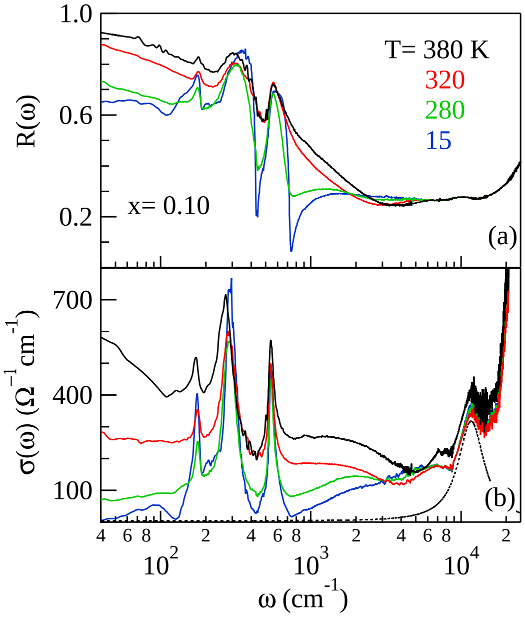

FIG. 6: (Color online) Reflectivity (a) and optical conductivity (b) of $\mathrm{Sr_{0.90}Ce_{0.10}MnO_3}$ at four temperatures. In b), the 1.5 eV band is shown as provided by a Lorentzian fit.

binding energy [10] of $\sim$ 0.1 eV should be subtracted to the peak energy of A, thus providing in Eq. 1 $E_{JT}/2 \sim 0.2$ eV for a $\mathrm{Mn^{3+}}$ ion in a matrix of $\mathrm{Mn^{4+}}$.

The optical response of the $x = 0.10$ sample is shown in Fig. 6-a and -b in terms of $R(\omega)$ and $\sigma(\omega)$, respectively, up to 380 K, well in the PM phase. Besides the phonon lines, a pronounced peak appears in $\sigma(\omega)$ at 12000 cm^{-1} or 1.5 eV. Its shape is also shown as provided by a Lorentzian fit. This contribution, which at $x = 0.05$ is not resolved from the O-Mn charge-transfer but is required by the fit, is also clearly seen in $\mathrm{SrMnO_3}$ [27]. Bands at 1.5 eV were observed in several hole-doped manganites, and assigned to $e_g - e_g$ transitions of different kind according to different authors. They were proposed to occur within the $\mathrm{Mn^{3+}}$ ions [28], or in inter-site jumps with either $\vec{s}$ and $\vec{S}_j$ antiparallel [14] or parallel [7]). However, the band at 1.5 eV here appears at low or even zero doping [27], where there are no $\mathrm{Mn^{3+}}$ ions. Moreover, 1.5 eV appears to be much higher than the expected Jahn-Teller splitting $e_g - e_g$, which should be on the scale of the lattice excitations. Therefore, also in agreement with Ref. 16, it seems reasonable to assign the 1.5 eV band to the $t_{2g} - e_g$ crystal field splitting Δ_{CF} in Eq. 2.

The subtraction procedure described above, when applied to the mid-infrared absorption of $x = 0.10$ (Fig. 7) shows again two bands A and B, with A which transfers most of its spectral weight to B below T_N. Therefore, as in the 0.05 sample, magnetic polarons should be present in the PM phase at x 0.10. They are expected to have a lower binding energy than at 0.05. Indeed, magnetic and dc resistivity measurements on $\mathrm{Ca_{1-x}La_xMnO_3}$ for $x \lesssim 1$ show that the polaron energy may decrease by an order of magnitude as x increases [29]. This is fully consistent with Fig. 7, where A is peaked at 1700-2000 cm^{-1} (depending on T). This corresponds to the bare $E_{JT}/2 = 0.2$ eV measured for $x = 0.05$, with a negligible correction for the energy of the magnetic polaron. B is peaked instead at 6500 cm^{-1} or 0.8 eV. In ϵ_2, both bands are well represented at any T by Lorentzians which, in terms of $\sigma(\omega)$, are shown at 320 K in the same Figure.

The spectral weights W_A and W_B change with temperature as shown in Fig. 8. A comparison with the $\chi(T)$ of Fig. 2-b shows a transfer of spectral weight between the two bands around $T_N = 295$ K, even if much less pronounced than for $x = 0.05$. Indeed at $x = 0.10$ both bands are present also below T_N, with $W_A/W_B \simeq 1/3$. This is consistent with the 0.10 system being in a phase of type C instead of G. Basing only on the spin population ratio in a C-type phase one would obtain $W_A/W_B = 1/2$. However, the dipole matrix elements cannot be the same

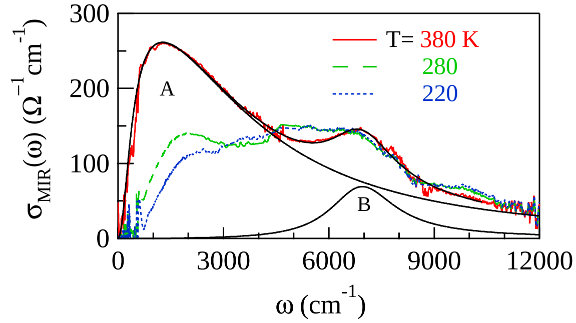

FIG. 7: (Color online) The optical conductivity of $\mathrm{Sr_{0.90}Ce_{0.10}MnO_3}$ is subtracted of the contributions in the far infrared (Drude, phonon) and in the visible range. In the resulting mid-infrared absorption, a moderate transfer of spectral weight W from A to B is evident below $T_N = 295$ K. Lorentzian fits to both bands A and B (see text) are shown for $T = 380$ K.

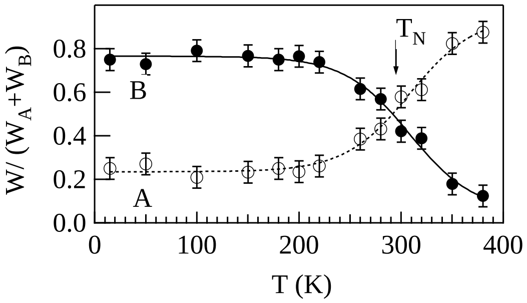

FIG. 8: Relative spectral weight vs. T, in $\mathrm{Sr_{0.90}Ce_{0.10}MnO_3}$, of the A (circles) and B bands (dots) of Fig. 7. The lines are guides to the eye and the arrow indicates the Néel temperature extracted from Fig. 2.

for $i-j$ hopping with $\vec{s}$ and $\vec{S}_j$ parallel and antiparallel, as the final states are different. Also partial charge ordering, as that observed in $\mathrm{Nd}_{1-x}\mathrm{Sr}_x\mathrm{MnO}_3$ for $x > 0.3$ [22], might affect W_A/W_B through an anisotropic distribution of the 10% Mn^{3+} ions. For example, if the latter ions were distributed preferentially along the c axis, where the ion spins are parallel, part of the transitions which produce band A would become Mn^{3+} - Mn^{3+}. They would then move to much higher energies, due to the Hubbard repulsion, making $W_A/W_B < 1/2$.

One can now determine the energies involved in the electron hopping. Both $E_{JT} \sim 0.4$ eV, on the scale of lattice excitations as expected, and $\Delta_{CF} \simeq 1.5$ eV, are measured directly. The Hund's splitting can then be found using Eq. 2. One finds $J_H S$ = 0.9 - 0.2 + 1.5 = 2.2 eV for $x = 0.05$, $J_H S$ = 0.8 - 0.2 + 1.5 = 2.1 eV for x = 0.10. Within the 10 % uncertainty of the experiment both samples provide the same value, which also falls in the range calculated in Ref. 11 for a $t_{2g} - t_{2g}$ Hund's splitting. If instead the lowest final state with antiparallel spin were e_g, one would obtain $J_H S = 0.7$ (0.6) eV for $x = 0.05$ (0.10). These values, however, would be much lower than usually expected for the Hund's splitting.

In conclusion, we have directly observed the dramatic change of the mid-infrared optical conductivity induced by the onset of the Hund's mechanism at the PM-AFM transition. The effect, so clearly observed for the use of an electron system at high dilution, allowed us to determine E_{JT}, Δ_{CF}, and $J_H S$ with good accuracy. The present study has also shown that, in a PM phase at high Mn^{3+} dilution, the hopping charge can move in a locally ferromagnetic lattice, *i. e.*, as a magnetic polaron.

Acknowledgments

We wish to thank A. J. Millis and M. Grilli for useful discussions.

[1] C. Zener, Phys. Rev. **82**, 403 (1951).

[2] P. W. Anderson and H. Hasegawa, Phys. Rev. **100**, 675 (1955).

[3] A. J. Millis, B. I. Shraiman, and R. Mueller, Phys. Rev. Lett. **77**, 175 (1996).

[4] A. Nucara, A. Perucchi, P. Calvani, T. Aselage, J. A. Voigt and D. Emin, Phys. Rev. B **6**8, 174432 (2003).

[5] K. H. Kim, J. H. Jung, and T. W. Noh, Phys. Rev. Lett. **81**, 1517 (1998).

[6] A. V. Boris, N. N. Kovaleva, A. W. Bazhenov, P. J. M. Van Bentum, Th. Rasing, S- W. Cheong, A. V. Samoilov, and N.-C. Yeh, Phys. Rev. B **59**, R697 (1999).

[7] M. Quijada, J. Cerne, J. R. Simpson, H. D. Drew, K. H. Ahn, A. J. Millis, R. Shreekala, R. Ramesh, M. Rajeswari, and T. Venkatesan, Phys. Rev. B **58**, 16093 (1998).

[8] K. H. Ahn and A. J. Millis, Phys. Rev. B **61**, 13545 (2000).

[9] S. Fratini, D. Feinberg, and M. Grilli, Eur. Phys. J. B **22**, 157 (2001).

[10] H. Meskine, T. Saha-Dasgupta, and S. Satpathy, Phys. Rev. Lett. **92**, 056401 (2004).

[11] S. Satpathy, Zoran S. Popovic, and Filip R. Vukajlovic, Phys. Rev. Lett. **76**, 960 (1996).

[12] E. Dagotto, T. Hotta, and A. Moreo, Phys. Rep. **344**, 1 (2001).

[13] Z. Fang, I. V. Solevyev, and K. Terakura, Phys. Rev. Lett. **84**, 3169 (2000).

[14] Y. Okimoto, T. Katsufuji, T. Ishikawa, T. Arima, and Y. Tokura, Phys. Rev. B **55**, 4206 (1997).

[15] J. H. Jung, K. H. Kim, D. J. Eom, T. W. Noh, E. J. Choi, Jaejun Yu, Y. S. Kwon, and Y. Chung, Phys. Rev. B **55**, 15489 (1997).

[16] N. N. Kovaleva, A. V. Boris, C. Bernhard, A. Kulakov, A. Pimenov, A. M. Balbashov, G. Khaliullin, and B. Keimer, Phys. Rev. Lett. **93**, 147204 (2004).

[17] A. Sundaresan, J. L. Tholence, A. Maignan, C. Martin, M. Hervieu, B. Raveau, and E. Suard, Eur. Phys. J. B **14**, 431 (2000).

[18] J. Hemberger, A. Krimmel, T. Kurz, H.-A. Krung von Nidda, V. Yu. Ivanov, A. A. Mukhin, A. M. Balbashov, and A. Loidl, Phys. Rev. B **66**, 094410 (2002).

[19] P. Mandal, A. Hassen, and A. Loidl, Phys. Rev. B **69**, 224418 (2004).

[20] C. Martin, A. Maignan, M. Hervieu, B. Raveau, Z. Jirák, A. Kurbakov, V. Trounov, G. André, and F.Bourée, Phys. Rev. B **62**, 6442 (2000).

[21] Z. Jirak, S. Krupicka, Z. Simsa, M. Dlouhá, and S. Vratislav, J. Magn. Magn. Mater. **53**, 153 (1985).

[22] K. Tobe, T. Kimura, and Y. Tokura, Phys. Rev. B **69**, 014407 (2004).

[23] W. Bao, J. D. Axel, C. H. Chen, and S-W. Cheong, Phys. Rev. Lett. **78**, 543 (1997).

[24] K. Takenaka, S. Okuyama, S. Sugai, and M. Yu. Maksimuk, J. Phys. Soc. Jpn. **71**, 3065 (1997).

[25] M. Ortolani, S. Lupi, P. Calvani, and P. Maselli, J. Opt. Soc. Amer. B **22**, 1994 (2005).

[26] N. N. Loshkareva, L. V. Nomerovannaya, E. V. Mostovshchikova, A. A. Makhnev, Yu. P. Sukhorukov, N. I. Solin, T. I. Arbuzova, S. V. Naumov, N. V. Kostromitina, A. M. Balbashov, and L. N. Rybina, Phys. Rev. B **70**, 224406 (2004).

[27] A. Sacchetti, M. Baldini, F. Crispoldi, P. Postorino, P. Dore, A. Nucara, C. Martin, and A. Maignan, unpublished.

[28] J.H. Jung, K. H. Kim, T. W. Noh, E. J. Choi, and Jaejun Yu, Phys. Rev. B **57**, R11043 (1998).

[29] J.J. Neumeier and J. L. Cohn, Phys. Rev. B **61**, 14319 (2000).